

Dark-field imaging is demonstrated with a conventional hard-x-ray source

Until now x-ray images with the revealing contrast afforded by dark-field techniques could only be gotten at synchrotron light sources.

In optical microscopy, dark-field imaging is a well-established means of enhancing contrast. By diverting most of the illuminating light before it reaches the focal plane and imaging only with light that scattered within the sample, one can highlight small scattering inhomogeneities that are hard to discern in the glare of the illumination source.

One would like to do the same with x-ray imaging. Bone and some pathological tissues incorporate microscopic x-ray scattering sites that would provide much better contrast than one gets with conventional medical radiographs, which rely entirely on x-ray absorption. Dark-field x-ray imaging would also help security screening by distinguishing between microscopically homogeneous soft materials and similarly absorbing explosives like Semtex that incorporate telltale microgranule scatterers. And for safety inspection of materials, microfractured regions would reveal themselves as x-ray scatterers in a dark-field image.

The problem with x rays, and especially with the hard, multi-keV x rays needed to penetrate samples of reasonable thickness, is the lack of efficient optical elements that could function like lenses. In recent years crystal surfaces have begun to serve as efficient Bragg reflectors for dark-field imaging with hard x rays.1 But producing crystalbased dark-field images with practical exposure times requires extremely well-collimated monochromatic beams of a kind that are available only at very brilliant synchrotron light sourceshardly a practical way of doing routine medical or surveillance imaging.

But now, Franz Pfeiffer and coworkers at the Paul Scherrer Institute (PSI) in Switzerland have demonstrated a way of doing dark-field imaging with hard x rays from an ordinary laboratory source much like the x-ray tubes used in most hospitals.² The technique employs a pair of interferometer gratings fabricated by Christian David of the PSI group. Interferometry usually requires

the coherence provided by a pointlike monochromatic source. But an x-ray tube like the one used at PSI yields a beam with a broad energy spectrum centered around 30 keV that cannot be focused down to a point much smaller than a square millimeter.

Therefore Pfeiffer and company covered the focus of the x-ray beam with a much coarser third grating (G_0 in figure 1a) that imposed a vertically striated

modulation with a periodicity of 73 μ m on the beam. That modulation just after the x-ray source suffices to provide the effective coherence in the transverse x direction required for the much finer phase-modulation and analyzer-absorption gratings (G_1 and G_2 in the figure) downstream of the sample to imprint interferometric information about its distribution of scatterers on the imaging detector.

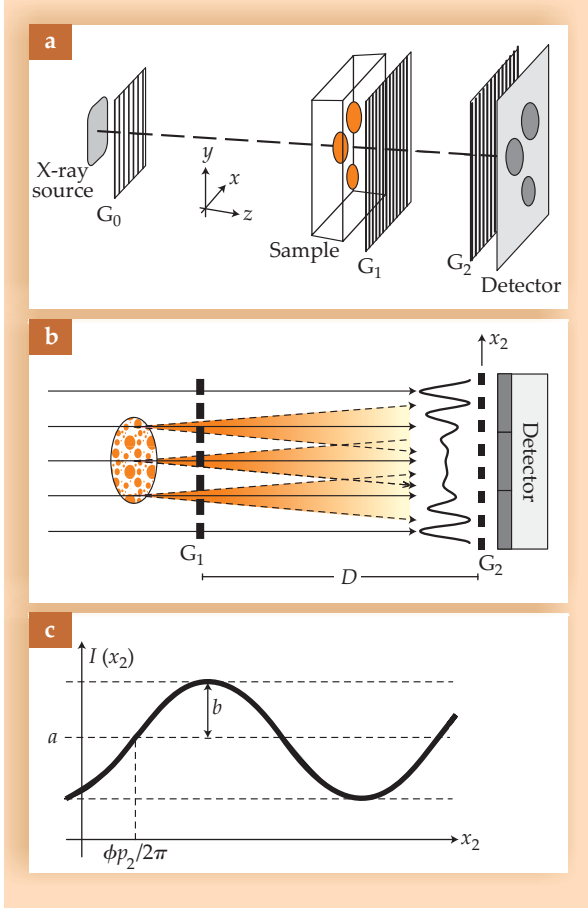


Figure 1. X-ray grating interferometer used to demonstrate dark-field imaging with a conventional 40-kV x-ray source.2 (a) A coarse diffraction grating G₀ covers the source. Just beyond the sample being imaged is G₁, a much finer phasemodulating grating with a period of 4 μ m. In front of the x-ray detector is the analyzerabsorption grating G₂, whose period is half that of G_1 . (b) Phase modulation by G₁ produces an oscillatory intensity pattern of inter-ference fringes in the plane of G_2 with half the period of G_1 . Smallangle x-ray scattering in the sample tends locally to wash out the fringes. Scanning G₂ across the detector and recording the resulting intensity oscillation at each detector pixel reveals the distribution of scatterers. (c) The recorded oscilla-

tion of the intensity I at any one pixel is, to good approximation, a sinusoidal function of G_2 's scanning position x_2 , with a period p_2 of 2 μ m. The smaller the oscillation amplitude b relative to the mean intensity a, the greater is the local scattering power in the sample. The distribution of phase angles ϕ can yield complementary image-contrast information. (Adapted from ref. 2.)

Revealing microscatterers

The PSI detector is limited by its pixel structure to a resolution on the order of 0.1 mm, far too coarse to resolve the micron-sized scatterers of interest. But their effect on the interferometric pattern produced at the detector by the gratings G_1 and G_2 shows up quite clearly in the group's dark-field images.

Placed just downstream of the sample, G_1 is a phase mask that imparts to the transmitted x-ray wavefront a phase modulation with a period p_1 of $4~\mu m$. By an interference phenomenon known in optics as the fractional Talbot effect, that phase modulation produces an intensity modulation with precisely half the period of G_1 at a distance D=4 cm farther downstream (see figure 1b). So that's where Pfeiffer and company placed their analyzer-absorption grating G_2 , with a period p_2 of 2 μm , followed immediately by the pixelated detector.

In the absence of the intervening sample, the intensity modulation just before G_2 would be neatly sinusoidal, with a period of 2 μ m. But the interference pattern tends to be washed out locally by small-angle x-ray scattering in the sample. The trick, then, is to deduce the distribution of microscatterers in the sample from their reduction of spatial oscillation amplitude at different points on the detector.

To that end, the group scans G_2 , with its opaque striations, across the face of the detector for a few oscillation periods. The data recorded during the scan are the set of x-ray intensities $I(m,n,x_2)$, where m and n index the detector's rectangular array of some 10^5 pixels and x_2 marks the progress of G_2 as it steps in the x direction in increments of $p_2/4$.

After the G_2 scan, the x_2 dependence of the x-ray intensity recorded by each pixel is Fourier analyzed. If one ignores the small contributions of higher harmonics of the fundamental oscillation period p_2 , each Fourier analysis yields the three-parameter fit

$$I(m,n,x_2) \approx a(m,n) + b(m,n)\sin[2\pi x_2/p_2 - \phi(m,n)]$$

(see figure 1c). When the fitted parameters are normalized to measurements made with the sample absent, the mean intensities a(m,n) correspond to what's recorded in a conventional x-ray radiograph, which exploits only absorption. The phases $\phi(m,n)$ are what one exploits in phase-sensitive x-ray imaging, a complementary alternative to darkfield imaging (see reference 3 and the article by Richard Fitzgerald in PHYSICS TODAY, July 2000, page 23). The darkfield imaging information is carried by

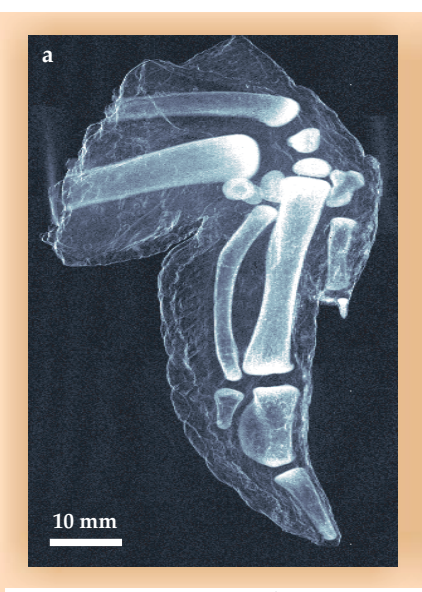




Figure 2. X-ray images of a chicken wing. **(a)** Dark-field image is a pixel-by-pixel plot of the visibility function V of the interference fringes at the detector in figure 1. The pixels are 0.2 mm on a side. Local small-angle scattering in the sample reduces V, which is a measure of the amplitude of interference oscillation. Pixels with the greatest reduction of V are shown brightest. Bones and interfaces, being sites of strong scattering, show with much better contrast than they do in **(b)**, which is a simulation of a conventional absorption-based radiograph produced from the same raw data that yielded the dark-field image. (Adapted from ref. 2.)

the visibility function

$$V(m,n) \equiv b(m,n)/a(m,n),$$

which measures the fractional depth of the interferometric oscillation.

The visibility function for a given pixel is an inverse measure of the local small-angle scattering power integrated over the projection of the pixel through the sample. The visibility of the oscillation at a point on the detector plane is most effectively reduced by x-ray scattering through an angle of $p_2/2D$ in the sample. Because the 0.2-mm pixel width is a hundred times bigger than p_2 , one needn't worry about scattering events recorded in the wrong pixel.

Comparison

Figure 2a, the PSI group's dark-field image of a chicken wing, demonstrates the technique's potential for improved contrast in medical imaging. The image is a map of V(m,n) created from the fitted Fourier parameters. It effectively subtracts off the mean glare of unabsorbed, unscattered x rays from the source. In the blackest regions of the image, the visibility function is the same as it is with no sample, and the whitest regions are where V is most diminished by scattering in the sample. In the sense that figure 2a is an analytically processed construct based on several

interferometric exposures, it is a less direct dark-field image than one gets with crystal manipulation of an x-ray beam at an accelerator light source.

For comparison, figure 2b shows what amounts to a conventional x-ray transmission image of the same sample, derived from the fitted *a* parameters for the same exposures that yielded the dark-field image. The much better bone contrast in the dark-field image is attributed by Pfeiffer and company to the strongly scattering microstructure of the porous bones. Scattering at softtissue boundaries and interfaces also provides good contour contrast. But the apparent absence of significant scattering in the bulk of the soft tissue renders it largely invisible in the dark-field image, even though its x-ray absorption is clearly manifested in the conventional radiograph. That suggests a useful complementarity between the two imaging modalities.

The two images were produced with five-second x-ray exposures at each of eight different positions of the analyzer-absorption grating. Keeping a living sample adequately still for almost a minute is problematic. But, says Pfeiffer, this proof-of-principle demonstration was carried out with an antiquated second-hand x-ray tube. With a more up-to-date source—albeit still describable as

"ordinary"—and a thicker detector of higher quantum efficiency, he expects that exposure time can be cut a hundred-fold. In any case, the wide band-pass acceptance of the new grating-based method allows much shorter exposure times than crystal-based dark-field imaging would require with a spectrally broad x-ray source of comparable brightness.

Absorption of x rays decreases with increasing energy, and soft tissue is less absorbing than bone. Therefore con-

ventional clinical imaging of soft tissue—mammography, for example—is done with relatively low-energy hard x rays of about 30 keV to insure adequate absorption. But absorption and its attendant ionization are precisely what subjects the patient to radiation risk. Because dark-field imaging does not depend on absorption, it could be done with less hazardous 100-keV x rays. "That shouldn't be difficult," says Pfeiffer. "But it will require the fab-

rication of diffraction gratings thick enough to absorb the more penetrating high-energy x rays."

Bertram Schwarzschild

References

- See, for example, T. J. Davis et al., *Nature* 373, 595 (1995); L. E. Levine, G. G. Long, *J. Appl. Crystallogr.* 37, 757 (2004); and M. Ando et al., *Nucl. Instrum. Methods Phys. Res. A* 548, 1 (2005).
- 2. F. Pfeiffer et al., Nat. Mater. 7, 143 (2008).
- 3. F. Pfeiffer et al., Nat. Phys. 2, 258 (2006).

Elementary excitations in spin ice take the form of magnetic monopoles

A magnet has two poles—north and south. But in a frustrated magnetic state known as spin ice, the familiar magnetic dipole can split into two magnetic charges that independently diffuse around the crystal.

Ferromagnetism—the ability of materials such as iron to form permanent magnets—arises from the spontaneous alignment of atomic spins when atoms interact with each other. But some magnetic solids, especially ones that are geometrically frustrated, exhibit rich and complex effects of those interactions. The behavior of a solid depends not just

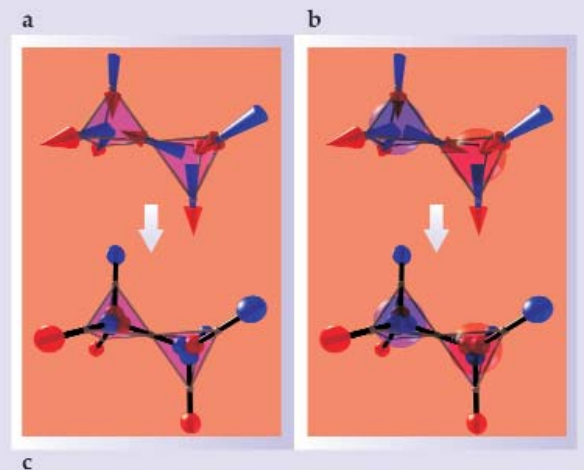
on the positions of its atoms but also on their local properties—the electric, magnetic, or rotational degrees of freedom. So when the energetically preferred alignment of magnetic moments in a lattice is incompatible with the underlying crystal geometry, exotic phases can emerge (see the article by Roderich Moessner and Art Ramirez in Physics TODAY, February 2006, page 24).

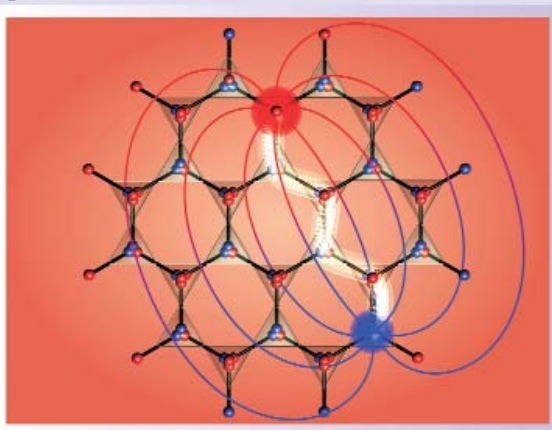
One of those phases, spin ice, is a strange magnetic state in a material whose ions reside on the vertices of the pyrochlore lattice, a network of cornersharing tetrahedra. A strong crystal field produced by the local environment of the ion favors an arrangement in which spins point either into or out of the cen-

ters of each tetrahedron. But as the temperature falls, geometric frustration inhibits the formation of a simple, ordered spin configuration in which every bond connects an in–out pair.

To minimize the energy, the best compromise is one in which two spins point into and two point out of each tetrahedron. That simple organizing principle, called an ice rule by analogy to the way hydrogen atoms are positioned around a central oxygen atom in water ice, can be satisfied by an exponentially large number of energetically equivalent arrangements of spins. The huge set of degenerate ground states is responsible for a characteristic property of spin ice: Although the material is structurally ordered, it remains magnetically disorderedand thus retains a residual, zero-point entropy—even as its temperature approaches absolute zero.

Claudio Castelnovo (Oxford University), Roderich Moessner (Max Planck Institute for the Physics of Complex Systems, Dresden), and





Mapping dipoles to dumbbells.

The magnetic moments in spin ice reside on the sites of the pyrochlore lattice, which consists of corner-sharing tetrahedra. The energy-minimizing ground states are described by the "ice rule": Two spins point out of each tetrahedron and two spins point in. (a) If the spin at each pyrochlore lattice site is stretched to span the centers of neighboring tetrahedra, with opposite magnetic charges at either end of a dumbbell, the ice rule is obeyed when the net charge of each tetrahedron is zero. (b) Inverting the shared spin in a pair of tetrahedra generates a monopole-antimonopole pair (the large red and blue balls). (c) As pictured in this slice of the pyrochlore lattice, thermal energy can prompt the oppositely charged monopoles to separate along a path (outlined in white) of adjacent tetrahedra. Once created at a finite temperature, the monopoles thus become independent, longlived topological defects in the crystal. Magnetic field lines connect the two monopoles. (Adapted from ref. 1.)